BRAIN COMMUNICATIONS

A potential role of fatty acid binding protein 4 in the pathophysiology of autism spectrum disorder

Motoko Maekawa,[1] Tetsuo Ohnishi,[1] Manabu Toyoshima,[1] Chie Shimamoto-Mitsuyama,[1] Kei Hamazaki,[2] (ID)Shabeesh Balan,[1] Yuina Wada,[1] Kayoko Esaki,[1] Shu Takagai,[3] Kenji J Tsuchiya,[4] Kazuhiko Nakamura,[5] Yasuhide Iwata,[6] Takahiro Nara,[7] Yoshimi Iwayama,[1] Tomoko Toyota,[1] Yayoi Nozaki,[1] Hisako Ohba,[1] Akiko Watanabe,[1] Yasuko Hisano,[1] Shigeru Matsuoka,[8] Masatsugu Tsujii,[9] Norio Mori,[6] Hideo Matsuzaki[10] and (ID)Takeo Yoshikawa[1]

Autism spectrum disorder is a neurodevelopmental disorder characterized by difficulties in social communication and interaction, as well as repetitive and characteristic patterns of behaviour. Although the pathogenesis of autism spectrum disorder is unknown, being overweight or obesity during infancy and low weight at birth are known as risks, suggesting a metabolic aspect. In this study, we investigated adipose tissue development as a pathophysiological factor of autism spectrum disorder by examining the serum levels of adipokines and other metabolic markers in autism spectrum disorder children ($n = 123$) and typically developing children ($n = 92$) at 4–12 years of age. Among multiple measures exhibiting age-dependent trajectories, the leptin levels displayed different trajectory patterns between autism spectrum disorder and typically developing children, supporting an adipose tissue-dependent mechanism of autism spectrum disorder. Of particular interest, the levels of fatty acid binding protein 4 (FABP4) were significantly lower in autism spectrum disorder children than in typically developing subjects, at preschool age (4–6 years old: $n = 21$ for autism spectrum disorder and $n = 26$ for typically developing). The receiver operating characteristic curve analysis discriminated autism spectrum disorder children from typically developing children with a sensitivity of 94.4% and a specificity of 75.0%. We resequenced the exons of the *FABP4* gene in a Japanese cohort comprising 659 autism spectrum disorder and 1000 control samples, and identified two rare functional variants in the autism spectrum disorder group. The Trp98Stop, one of the two variants, was transmitted to the proband from his mother with a history of depression. The disruption of the *Fabp4* gene in mice evoked autism spectrum disorder-like behavioural phenotypes and increased spine density on apical dendrites of pyramidal neurons, which has been observed in the postmortem brains of autism spectrum disorder subjects. The *Fabp4* knockout mice had an altered fatty acid composition in the cortex. Collectively, these results suggest that an 'adipo-brain axis' may underlie the pathophysiology of autism spectrum disorder, with FABP4 as a potential molecule for use as a biomarker.

1   Laboratory for Molecular Psychiatry, RIKEN Center for Brain Science, Saitama, Japan
2   Department of Public Health, Faculty of Medicine, University of Toyama, Toyama, Japan
3   Department of Child and Adolescent Psychiatry, Hamamatsu University School of Medicine, Shizuoka, Japan
4   Research Center for Child Mental Development, Hamamatsu University School of Medicine, Shizuoka, Japan
5   Department of Psychiatry, Hirosaki University School of Medicine, Aomori, Japan
6   Department of Psychiatry and Neurology, Fukude Nishi Hospital, Shizuoka, Japan
7   Department of Rehabilitation, Miyagi Children's Hospital, Miyagi, Japan
8   Department of Clinical Pharmacology, Faculty of Medicine, Oita University, Oita, Japan
9   School of Contemporary Sociology, Chukyo University, Aichi, Japan
10   Research Center for Child Mental Development, University of Fukui, Fukui, Japan
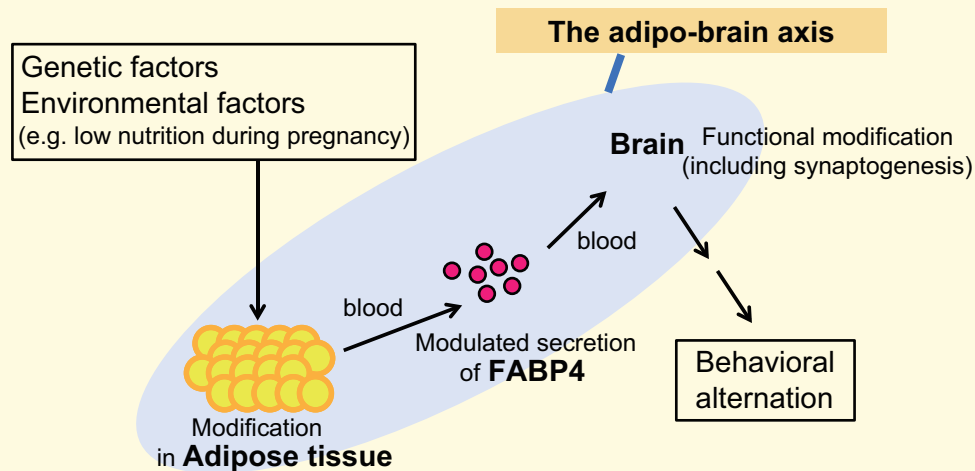
Correspondence to: Motoko Maekawa, Laboratory for Molecular Psychiatry, RIKEN Center for
Brain Science, 2-1 Hirosawa, Wako-city, Saitama 351-0198, Japan.
E-mail: motoko.maekawa@riken.jp

Correspondence may also be addressed to: Takeo Yoshikawa.
E-mail: takeo.yoshikawa@riken.jp

Graphical Abstract

Introduction

Autism spectrum disorder (ASD) is a neurodevelopmental disorder characterized by persistent difficulties in social communication and social interaction. The prevalence of ASD, now estimated to be 1–2%, is increasing annually (World Health Organization; https://www.who.int/news-room/fact-sheets/detail/autism-spectrum-disorders, last accessed 9 September 2020) (Weintraub, 2011; Lai *et al.*, 2014). Although ASD is thought to be caused by complex interactions between genetic and environmental factors, the detailed mechanism of the pathogenesis of ASD remains unclear (de la Torre-Ubieta *et al.*, 2016; Rylaarsdam and Guemez-Gamboa, 2019).

ASD children show various developmental differences compared with typically developing (TD) children in early childhood. For example, early brain overgrowth at 6–24 months of age has been frequently reported as a neuroanatomical feature of ASD children (Courchesne *et al.*, 2011). Another study reported on the aberrant development of white matter tracts in the first year of life of ASD children (Wolff *et al.*, 2012). In addition to brain development, ASD children present several characteristics relevant to the lipid metabolism, particularly in early development. Adipose tissue secretes hundreds of bioactive molecules (adipokines) (Luo and Liu, 2016), some of which modulate brain functions (Parimisetty *et al.*, 2016).

ASD children show changes in the levels of adipokines, including increased leptin levels (Ashwood *et al.*, 2008; Blardi *et al.*, 2010), decreased adiponectin levels (Fujita-Shimizu *et al.*, 2010) and increased monocyte chemotactic protein-1 (MCP-1) levels (Ashwood *et al.*, 2011) in early childhood.

Fatty acid binding protein 4 (FABP4, also known as adipocyte-FABP or aP2), a member of the FABP family (Zimmerman and Veerkamp, 2002), is thought to form a complex with fatty acids (FAs) (Gillilan *et al.*, 2007) and functions as a chaperone for FAs within cells (Furuhashi and Hotamisligil, 2008). FABP4 was recently identified as a novel adipokine and may play a role as an adipokine in the pathology of metabolic syndromes (Furuhashi and Hotamisligil, 2008; Prentice *et al.*, 2019). In our previous study, *FABP4* expression was found to decrease in the scalp hair follicles of patients with schizophrenia (Maekawa *et al.*, 2015). However, to date, the relationship between FABP4 and autism has not been investigated.

In this study, we systematically measured the serum levels of various adipokines, including FABP4, in subjects aged 2–12 years (preschool to elementary school age) and found that serum FABP4 levels were reduced in ASD children at the preschool stage. Based on these results, we further investigated a possible link between the pathogenesis of ASD and the functional disturbance of FABP4

by leveraging human genetics and analysis of gene-deficient mice.

Materials and methods

Human serum samples

All subjects were Japanese living in central or eastern Japan, including the Hokuriku, Chubu, Tokai, Kanto and Tohoku regions. The clinical diagnosis of ASD was made by board-certified child psychiatrists based on the Diagnostic and Statistical Manual of Mental Disorders, fourth edition, text revision (American Psychiatric Association, 2000) using the information of developmental history. The ASD diagnosis was confirmed by a structured developmental interview with the subject's parents (Autism Diagnostic Interview-Revised) (Lord *et al.*, 1994; Le Couteur *et al.*, 2008; Falkmer *et al.*, 2013). One of the authors (K.J.T.) previously attended an Autism Diagnostic Interview-Revised research training workshop and established research reliability with Weill Cornell Medicine Psychiatry. The ethics committees of the participating institutes approved the study protocols, and written informed consent was obtained from the parents of all participants. The current study was conducted in accordance with the Declaration of Helsinki.

The first sample set included 102 ASD and 87 TD children, which were divided into a preschool-aged group (4–6 years old) (ASD: 18 men, 3 women; mean age, 5.70 ± 0.96 years; TD children: 14 men, 12 women, mean age 6.05 ± 0.64 years) and an elementary school-aged group (7–12 years old) (ASD: 93 men, 9 women, mean age 10.08 ± 1.55 years; TD children: 55 men, 11 women, mean age 10.47 ± 1.70 years) (Supplementary Table 1). The second sample set included 21 ASD (2–4 years old) (14 men, 7 women; mean age, 3.79 ± 0.74 years) and 24 TD children (2–4 years old) (13 men, 11 women; mean age, 3.72 ± 0.82 years) (Supplementary Table 2). Fasting blood samples were collected between 6:00 and 9:00 by venipuncture from all the participants, and the samples were kept at room temperature for 30 min. They were then centrifuged, divided into 200-μl aliquots and stored at $-80°C$ until use.

Measurement of adipokines and metabolic biomarkers in serum samples

Serum FABP4 concentrations were measured using enzyme-linked immunosorbent assay (ELISA) kits (Cayman Chemical, Ann Arbor, MI, USA). Levels of insulin, MCP-1, and leptin were measured using Multiplex Assay kit 'Human Metabolic Disease Panel' (Merck Millipore, Darmstadt, Germany). The adiponectin levels were determined using sandwich ELISA kits (R&D Systems Inc., Minneapolis, MN, USA), according to the manufacturer's instructions. The glucose concentrations were measured using a commercial kit (Glu-CII; Wako Pure Chemical Industries, Ltd., Osaka, Japan). The levels of free fatty acid were measured using a Free Fatty Acid Fluorometric Assay Kit (Cayman Chemical). Each serum sample was analysed in duplicate, and the mean value of the two measures was used for analysis.

DNA samples

DNA samples were collected from Japanese subjects who were born and living in central Japan separately from the serum samples. ASD was diagnosed based on the Autism Diagnostic Interview-Revised . Control subjects were recruited from volunteers with no present or previous evidence of psychosis during brief interviews by psychiatrists. The DNA sample set comprised 659 subjects with ASD (529 men, 130 women; mean age, 12.13 ± 7.82 years) and 1000 controls (500 men, 500 women; mean age 41.40 ± 14.37 years).

Re-sequencing analysis of *FABP4*

All coding exons and exon/intron boundaries of the *FABP4* gene were screened for polymorphisms by direct sequencing using the BigDye Terminator v3.1 Cycle Sequencing kit (Applied Biosystems, Foster City, CA, USA) and an ABI 3730xl sequencer (Applied Biosystems). Polymorphisms were detected using SEQUENCHER software (Gene Codes Corporation, Ann Arbor, MI, USA) (Balan *et al.*, 2014). The genomic structure of *FABP4* (RefSeq: NM_001442.2) was based on the UCSC hg19 draft assembly of the human genome database (http://www.genome.ucsc.edu, last accessed 9 September 2020). The NCBI database (https://www.ncbi.nlm.nih.gov/snp/, last accessed 9 September 2020) was searched for known single nucleotide polymorphisms (SNPs).

Construction of plasmids

Human *FABP4* cDNA was obtained by PCR using Human Fetal Brain Marathon-Ready cDNA (Clontech, Mountain View, CA, USA) and the following primer set: forward: 5′-ATTGAATTCATGTGTGATGCTTTTGTA-3′, reverse: 5′-TGAGTCGACTTATGCTCTCTCATAAAC-3′. The amplified cDNA was cloned into the mammalian expression vector pcDNA3 (Invitrogen, Grand Island, NY, USA). The Thr8Ala mutant was created by conventional site-directed mutagenesis. For the bacterial expression construct, a PCR fragment from the pcDNA3-FABP4 construct was inserted into the bacterial expression vector pGEX-6P-3 (GE Healthcare Life Sciences, Tokyo, Japan) using XhoI/BamHI. The structures of the generated plasmids were validated by Sanger sequencing.

Recombinant FABP4 protein

Recombinant FABP4 proteins (WT and Thr8Ala) were obtained as reported previously (Shimamoto *et al.*, 2014). Briefly, the proteins were produced using *Escherichia coli* BL21 (DE3) (BioDynamics Laboratory Inc., Tokyo, Japan) and purified using glutathione sepharose 4B (GE Healthcare Life Sciences). After the GST moiety was removed by digestion with PreScission protease (GE Healthcare Life Sciences) on the beads, the resulting recombinant proteins were de-lipidated using a Lipidex1000 column (PerkinElmer, Waltham, MA, USA).

Binding assay

The fluorescent FABP ligand 1-anilinonaphthalene-8-sulfonic acid (ANS) was purchased from Cayman Chemical (Ann Arbor, MI, USA). Binding assays using ANS were based on a previously described procedure (Shimamoto *et al.*, 2014). Fluorescence was measured using a multi-label counter (excitation at 355 nm and emission at 460 nm) (Wallac 1420 ARVO MX-2; Perkin Elmer). The dissociation constant (Kd) values were calculated by non-linear regression analysis using GraphPad Prism software (version 8, GraphPad Software, San Diego, CA, USA).

Animals

Fabp4-disrupted mice (gifted from Prof. Hotamışlıgil) were established as described in Hotamisligil *et al.* (1996) and maintained as a closed colony. The mice were maintained as a closed colony and heterozygotes were intercrossed to produce wild-type (WT) and *Fabp4*-null mice. The animals were housed in groups of four or five in standard cages in a temperature- and humidity-controlled room with a 12 h light/dark cycle (lights on at 08:00). The animals had free access to standard lab chow (CRF-1) (Charles River formula; purchased from Oriental Yeast, Tokyo, Japan) and tap water. All animal experiments were performed using male animals (7–16 animals/group, depending on the experiment). The experimental procedures were approved by the RIKEN Animal Ethics Committee (permission number: H30-B030139).

Behavioural analyses

The behavioural profiles of the *Fabp4* KO mice were assessed using the three-chamber social interaction, Morris water maze, and other behavioural tests at 6 weeks to 6 months, as well as with ultrasonic vocalization tests at postnatal day 5 (P5) to P14. The protocols for behavioural tests were as described in the Supplementary Methods and the literature (Ohnishi *et al.*, 2010; Shimamoto *et al.*, 2014).

Spine analysis

Mice were deeply anaesthetized with isoflurane and perfused transcardially with 4% paraformaldehyde in phosphate-buffered saline (PBS). The brains were trimmed and cut into 200-μm thick coronal sections using a vibratome. Lipophilic dye (DiI, Invitrogen) was coated onto tungsten particles (Bio-Rad, Hercules, CA, USA). DiI-coated particles were delivered to the slices using the Helios Gene Gun system (Bio-Rad). A polycarbonate filter with 8.0-μm pores (Beckton Dickinson, Franklin Lakes, NJ, USA) was inserted between the gun and the preparation to remove clusters of large particles. The density of labelling was regulated via gas pressure (95–105 psi helium) (Mataga *et al.*, 2004). A confocal laser-scanning microscope FV1000 (Olympus, Tokyo, Japan) was used to image the labelled structures. Randomly labelled typical pyramidal neurons were selected from layers II–III and V in the temporal cortex. Images at 0.45-μm steps were acquired and stacked for 3D reconstruction using ImageJ (https://imagej.nih.gov/ij/, last accessed 9 September 2020) and Spiso-3D (mathematical and automated software calculating geometrical parameters of spines) (Mukai *et al.*, 2011). Spines were counted along an apical dendrite for each neuron in eight mice per group. Spine density on apical dendrites was averaged at 50–100-μm from the cell body (Hutsler and Zhang, 2010).

Fatty acid analysis

Tissue samples were homogenized in ice-cold saline, and aliquots were used for lipid analysis. Total lipids were extracted according to the method described by Bligh and Dyer (1959). Total phospholipid fractions were separated by thin-layer chromatography. After transmethylation with HCl-methanol, the FA composition was analysed by gas chromatography (GC-2014; Shimadzu Corporation, Kyoto, Japan) with a DB-225 capillary column (length, 30 m; internal diameter, 0.25 mm; film, 0.25 μm; J&M Scientific, Folsom, CA, USA). The entire system was controlled using gas chromatography software GC-solution version 2.3 (Shimadzu Corporation). Each FA was expressed as a percentage of the total FA content.

Data availability

The data supporting these findings are available upon request.

Statistical analysis

The data were analysed using Prism 8 or SPSS version 16 (SPSS Inc., Chicago, IL, USA). Continuous data are expressed as median and range or mean ± standard error (SE). Outliers were removed based on the 1.5× interquartile range (IQR) rule. Statistical analyses were performed using the Mann–Whitney U test for mean differences and the Spearman rank test for correlation. $P < 0.05$ was considered significant.

Results

Serum levels of adipokines in childhood

The demographic data of the participants are summarized in Supplementary Table 1. No significant differences in age, intelligence quotient, weight, height, body mass index (Supplementary Table 1) or blood biochemical markers were found between the ASD and TD groups (Supplementary Table 3) in the all-age group and in each specific age group.

We measured the serum levels of adipokines which have been reported to be altered in ASD, including leptin, adiponectin and MCP-1 (Ashwood et al., 2008; Blardi et al., 2010; Fujita-Shimizu et al., 2010; Ashwood et al., 2011), except for FABP4, which, to the best of our knowledge, was first examined here. We also measured other metabolic parameters (insulin, glucose and free fatty acid) in the sera of ASD and TD children. The FABP4 and MCP-1 levels were negatively correlated with age in TD children, but not in ASD children (Fig. 1A and B). Leptin levels were positively correlated with age in ASD children but not in TD children (Fig. 1C). Adiponectin and free fatty acid levels were negatively correlated with age (Fig. 1D–G), while insulin and glucose levels were positively correlated with age in both the TD and ASD groups. Leptin level trajectories showed a significant difference between the ASD and TD groups in terms of the Spearman's correlation coefficients, while the other measures did not (Fig. 1H).

Considering the age-dependent changes in the levels of the above molecules, we divided the cohort into two groups: preschool-aged (4–6 years old) and elementary school-aged (7–12 years old) groups, and compared the mean levels of the molecules between the ASD and TD groups (Supplementary Table 1). In the preschool-aged group, the levels of FABP4 in ASD children were significantly lower than those in TD children (Fig. 1H), however, the levels of other molecules did not differ significantly between the ASD and TD groups (Supplementary Fig. 1). In the elementary school-aged group, the levels of MCP-1 and free fatty acid were significantly higher in the ASD group than in the TD group, but the levels of other markers were not significantly different between the ASD and TD groups (Supplementary Fig. 2).

FABP4 as an early biomarker of ASD

Since the early diagnosis and early intervention of ASD are important for prognosis (Lai et al., 2014) and the FABP4 levels in ASD children were low, specifically at the preschool stage (Fig. 1H), we subsequently focused on FABP4 and evaluated its potential as an early diagnostic biomarker. A receiver operating characteristic curve analysis determined the cut-off level at 16.7 ng/ml (Fig. 1I). The sensitivity, specificity, positive predictive values and negative predictive values were 94.4%, 75.0%, 5.6% and 25.0%, respectively. We did not observe any correlations between the levels of FABP4 and the psychological scores on ASD (intelligence quotient and items in Autism Diagnostic Interview-Revised) (Supplementary Table 4). The levels of FABP4 did not differ between the male and female samples (Supplementary Table 5). The serum levels of FABP4 are associated with obesity (Aeberli et al., 2008; Krzystek-Korpacka et al., 2011; Dencker et al., 2017). However, we found no correlations between the levels of FABP4 and physical indices (body mass index, height and weight) (Supplementary Table 6).

To determine whether the serum level of FABP4 could serve as a useful biomarker in the earlier stage, we examined the second set of samples at the toddler stage (2–4 years old), consisting of 21 ASD and 24 TD children (Supplementary Table 2). Again, the FABP4 levels were significantly lower in ASD children than in TD children (Fig. 1J). A receiver operating characteristic curve determined the cut-off level at 12.7 ng/ml. The sensitivity, specificity, positive predictive values and negative predictive values were 81.0%, 71.4%, 19.1% and 28.6%, respectively (Fig. 1K). These results demonstrate that the serum levels of FABP4 could be a versatile diagnostic biomarker for ASD at an early stage (at least 2–6 years old).

Exon resequencing analysis of the FABP4 gene

To search for a genetic underpinning of FABP4 abnormality seen in ASD, we conducted an exon resequencing analysis of the FABP4 gene using 659 ASD and 1000 control subjects. We identified one case with the missense mutation Thr8Ala and one case with the nonsense mutation Trp98Stop (Table 1 and Fig. 2A). FABP4 Thr8 is highly conserved among species and is located within a β-strand (Fig. 2B). The in silico web tool 'PolyPhen2' (http://genetics.bwh.harvard.edu/pph2/, last accessed 9 September 2020) estimates the possible impact of an amino acid substitution on the structure and function of the protein. This algorithm predicted that the FABP4 Thr8Ala mutation could be 'possibly damaging'. Pedigree samples were unavailable for this mutation. The FABP4 Trp98Stop mutation would result in the loss of 33 amino acids at the C-terminus, which is highly conserved and includes three β-strands (Fig. 2B) and three amino acids needed for FA binding (Cys118, Arg127 and Tyr129) (BioLiP database: https://zhanglab.ccmb.med.umich.edu/BioLiP/, last accessed 9 September 2020) (Supplementary Table 7). It is also possible that this transcript may be rapidly degraded by the nonsense-mediated mRNA decay system (Maquat, 2005; Behm-Ansmant et al., 2007; Kurosaki and Maquat, 2016). This mutation was
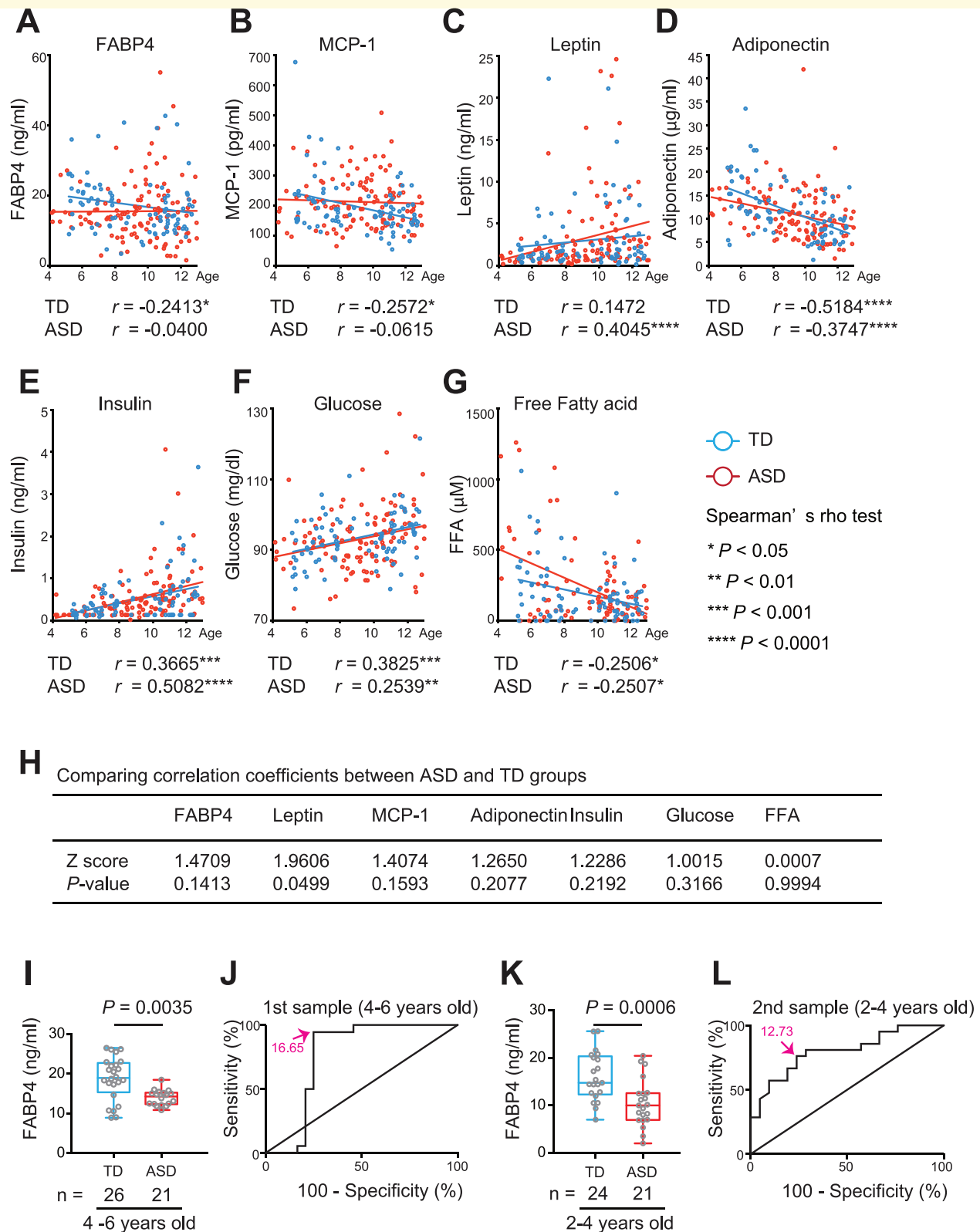
Figure 1 Serum levels of adipokines and other metabolic parameters in ASD and TD subjects. (**A**–**G**) Correlation between age and the levels of adipokines or other metabolic parameters: (**A**) FABP4, (**B**) leptin, (**C**) MCP-1, (**D**) adiponectin, (**E**) insulin, (**F**) glucose and (**G**) free fatty acids. (**H**) Comparison of correlation coefficients between ASD and TD groups. (**I**) FABP4 levels in ASD and TD groups of 4–6 years old. *P*-values were calculated using two-tailed Mann–Whitney *U* tests. (**J**) receiver operating characteristic curve for FABP4 at 4–6 years old. (**K**) FABP4 levels in ASD and TD groups at 2–4 years old. *P*-values were calculated using two-tailed Mann–Whitney *U* tests. (**L**) receiver operating characteristic curve for FABP4 at 2–4 years old.

Table 1 Polymorphisms identified in the FABP4 gene

Exon	Nucleotide change	Amino acid change	dbSNP ID	Autism (n = 516)	Control (n = 1000)
	c.1-6C>T		rs1585812890*	0	1
1	c.22A>G	Thr8Ala	rs1585812863*	1	0
3	c.294G>A	Trp98Stop	rs150131014*	1	0
4	c.399 + 11G>A		rs138590127*	0	3

Asterisks indicate newly identified SNPs. They were registered in the dbSNP (https://www.ncbi.nlm.nih.gov/snp/, last accessed 9 September 2020).

transmitted from his mother with a history of depression (Fig. 2C), suggesting that the mutation may co-segregate with psychiatric illnesses. The serum FABP4 level of the proband (12 years old) was 7.3 ng/ml, which is nearly half of the average levels of the TD group (14.4 ng/ml) and the ASD group (14.1 ng/ml) of the similar ages (elementary school ages) (Supplementary Fig. 2). These results suggest that although rare, there are ASD cases where FABP4 gene defects may be involved in the pathogenesis of ASD.

Binding property of the FABP4 mutant to the fluorescent ligand ANS

To investigate the biochemical effects of the FABP4 Thr8Ala variant, we measured the binding potential of the recombinant FABP4 mutant protein to 1-anilinonaphthalene-8-sulfonic acid (ANS). ANS is a fluorescent dye that binds with a high affinity to the ligand-binding pocket of the FABP proteins. In addition to the WT and the Thr8Ala mutant, we prepared a double mutant, FABP4 Arg107Ala/Arg127Ala, as a binding pocket-destructive mutant (Shimamoto et al., 2014). We were able to purify these proteins to an almost homogeneous level (Supplementary Fig. 3). We performed titration analyses of their affinities to the ANS (Fig. 2D). The dissociation constant (K_d) of the double mutant (FABP4 Ala107/ Ala127) to ANS was significantly higher than that of WT. In contrast, the K_d value of the Ala8 mutant to ANS was significantly lower than that of WT (Fig. 2E), demonstrating that the missense mutation increases the binding affinity to ANS, and probably to natural ligands such as fatty acids. However, the in vivo nature of the FABP4 Trp98Stop and Thr8Ala variants remains elusive.

Expression of FABP4 in postmortem brains

It has been reported that FABP4 is expressed in the human brain during both childhood (Human Brain Transcriptome, http://hbatlas.org/, last accessed 9 September 2020) and adulthood (Supplementary Fig. 4) (Maekawa et al., 2015). We examined the expression levels of FABP4 in postmortem brain samples from autistic subjects in Broadmann area 9 (control: $n = 10$, ASD: $n = 10$), Broadmann area 21 (control: $n = 14$, ASD:

$n = 14$), Broadmann area 40 (control: $n = 13$, ASD: $n = 14$) and dorsal raphe nucleus (control: $n = 8$, ASD: $n = 8$) (Supplementary Table 8). However, the expression of FABP4 was unchanged between the ASD and control groups in any brain region (Supplementary Fig. 4B). These results may correspond to the results in a Japanese cohort in which there were no significant differences in the FABP4 serum levels between the ASD and TD groups at the elementary school age. The ages of the postmortem brain samples ranged from elementary school ages and above. Extended brain samples, in terms of both age span and sample size, will need to be examined in a future study.

ASD-like behavioural phenotypes of Fabp4 KO mice

To investigate the effects of a functional disturbance of FABP4, we evaluated the behaviours of Fabp4 KO mice. The Fabp4 KO mice were healthy with no visible abnormalities in terms of growth or morphology. In the three-chamber test (Fig. 3A), a reduced exploratory behaviour toward a stranger mouse was observed in Fabp4 KO mice (Fig. 3B). In the Morris water maze test (Fig. 3C), Fabp4 KO mice exhibited reduced spatial learning and memory, represented by the lack of a clear increase in the time spent in the target quadrant (platform) or the number of times the target platform was crossed after training (Fig. 3D and E). This result may be related to the impaired visuospatial ability reported in individuals with ASD (McGrath et al., 2012; Habib et al., 2019). We did not observe significant differences in a reversal learning test between the Fabp4 KO and WT mice (data not shown), which evaluates a perseveration trait usually under the condition of non-impaired spatial learning ability. To evaluate the ability of verbal communication in Fabp4 KO mice, we examined the ultrasonic vocalization of the pups when they were separated from the dam at P5, P7, P10 and P14. While we found no significant differences in the number of calls between the WT littermates and Fabp4 KO mice at any stage (Fig. 3F), Fabp4 KO mice showed significant increases in the duration of total calls (Fig. 3G and H) and in several subtype calls (Supplementary Fig. 5A and B) at P5. We found that the ratio of calls with a peak frequency maximum above 90 kHz was elevated in Fabp4 KO mice compared to their WT littermates at P5 (Fig. 3I and Supplementary Fig. 5C). These findings are consistent with the report
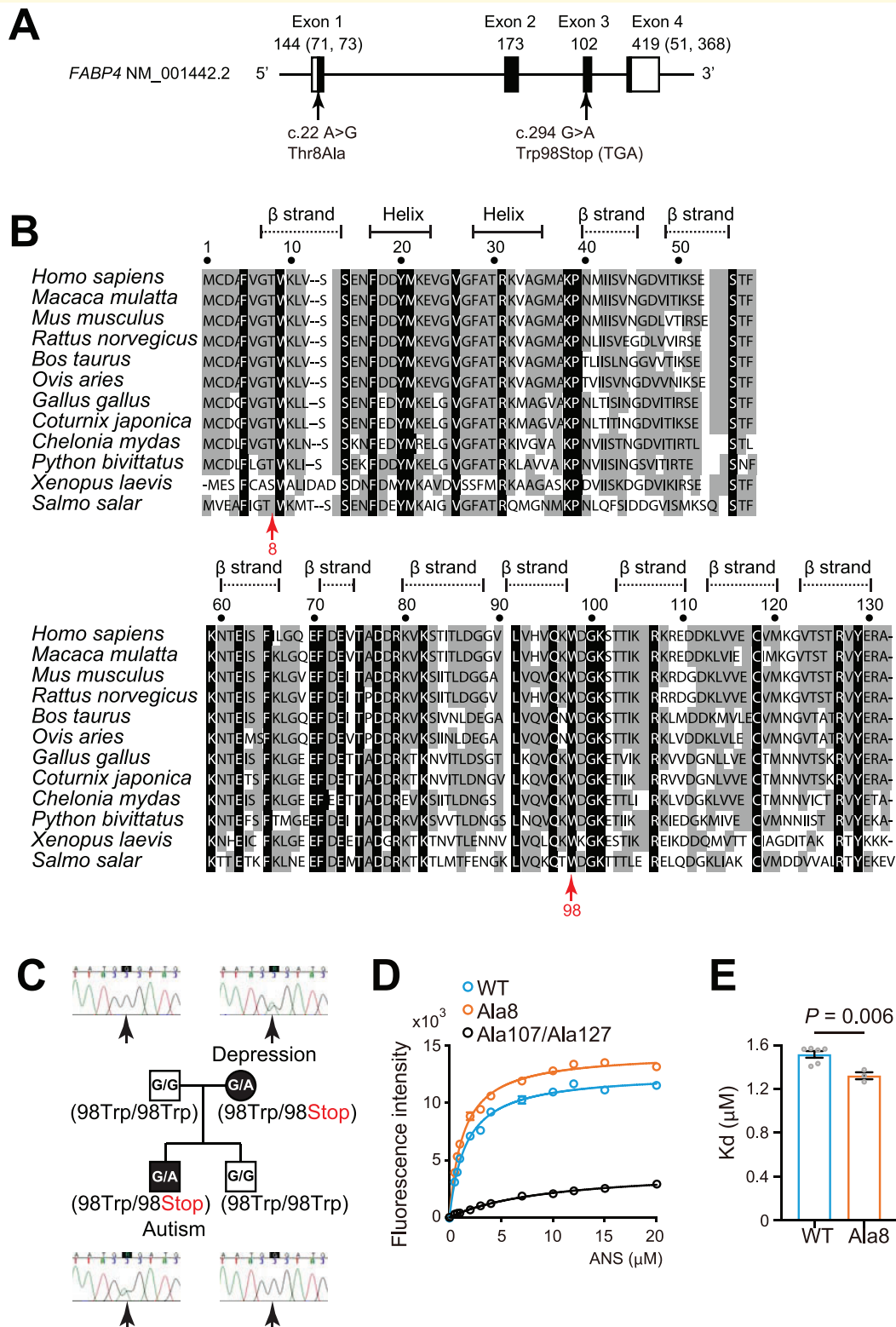
Figure 2 Exon resequencing analysis of the *FABP4* gene. (**A**) Gene structure of human *FABP4*. Exon is shown as a square, with the coding regions in black and the untranslated regions in white. Polymorphisms identified in ASD are indicated by arrows. (**B**) Amino acid sequence alignment of FABP4 between multiple species. Black boxes indicate amino acids conserved from Atlantic salmon (*Salmo salar*) to humans. The grey boxes indicate partially conserved amino acids. The variants identified in ASD are shown using arrows, with the amino acid positions. (**C**) Family structure of the proband with the *FABP4* Trp98Stop mutation. The black symbols represent individuals with the *FABP4* Trp98Stop mutation. The squares and circles indicate men and women, respectively. (**D**) ANS was incubated with recombinant FABP4 proteins and the intensity of fluorescence was recorded (excitation filter: 355 nm, emission filter: 460 nm). The data are representative of independent experiments. (**E**) Kd value obtained from ANS assays.
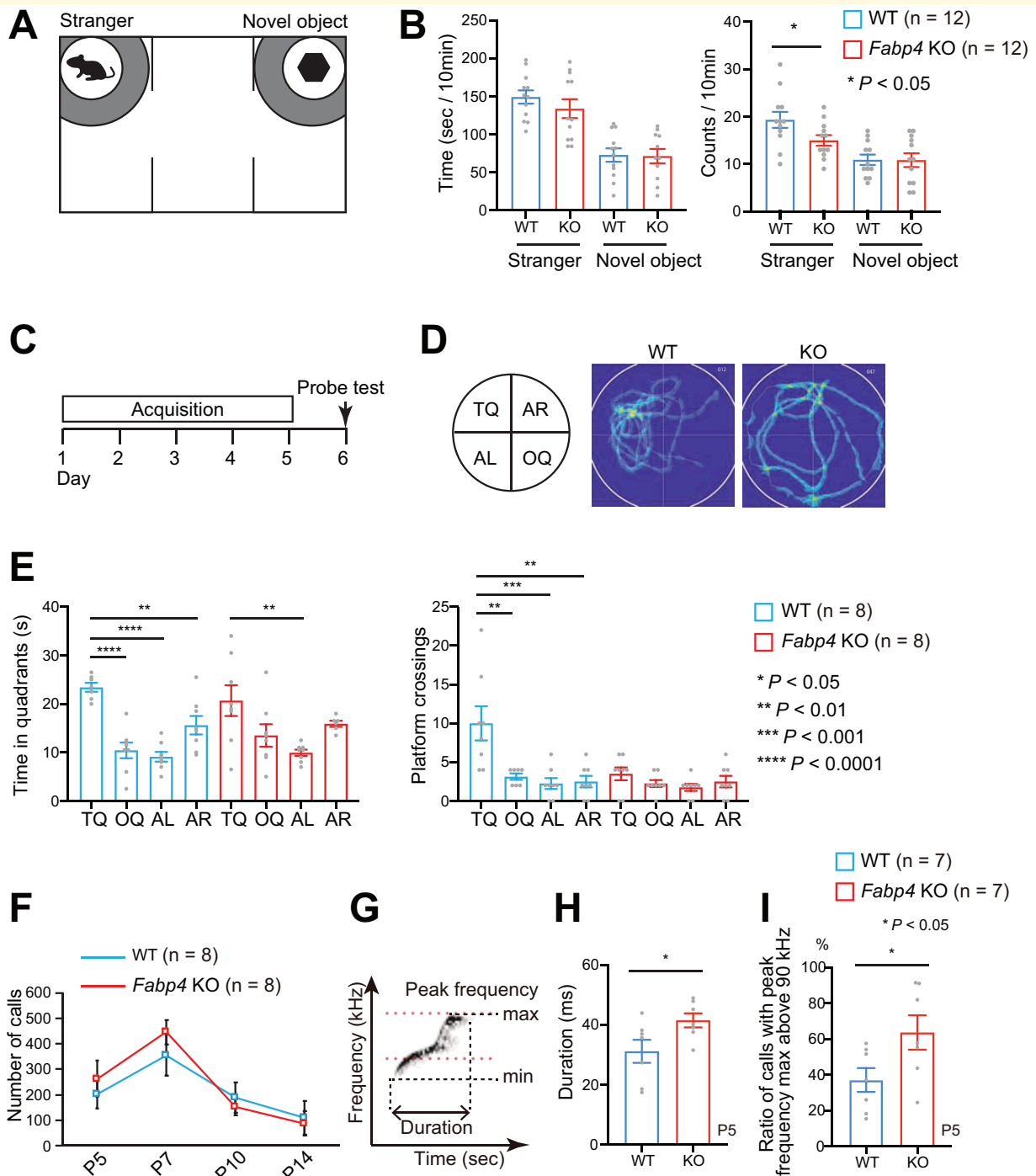
Figure 3 Behavioural analyses in *Fabp4* KO mice. (**A, B**) Three-chamber social behaviour test. (**A**) Schematic diagram of the equipment used in the three-chamber social behaviour test. (**B**) Left panel shows the total time spent in the stranger mouse area and the novel object area. Right panel shows the number of intrusions into the stranger mouse area and the novel object area. *P*-values were calculated using two-tailed Mann–Whitney *U* tests. (**C, D**) Morris water maze test. (**C**) The Morris water maze examination schedule. After 5 days of training, a probe test was performed. AL = adjacent left; AR = adjacent right (upper panel); OQ = opposite quadrant; TQ = target quadrant. In the lower panel, a representative example of the behavioural patterns exhibited by mice of each genotype during the 10 min of the study is shown. (**D**) The upper panel shows the total length of the stay (s) in each quadrant area during the probe test. The lower panel shows the number of times the quadrant area was crossed over during the probe test. *P*-values were calculated using one-way ANOVA, followed by *post hoc* Tukey's test. (**E–H**) Ultrasonic vocalization analysis of *Fabp4* KO pups. (**E**) Total number of calls at postnatal day 5 (P5), P7, P10 and P14. (**F**) Detailed spectral features of a call. (**G**) Average of duration of calls at P5. *P*-values were calculated using two-tailed Mann–Whitney *U* tests. (**H**) Ratio of calls above 90 Hz at P5. *P*-values were calculated using two-tailed Mann–Whitney *U* tests.

that crying in infants with ASD has relatively higher frequencies (Esposito *et al.*, 2017). No significant differences were observed in the other behavioural batteries (Supplementary Table 9). Collectively, *Fabp4* KO mice showed some behavioural phenotypes of ASD.

Increased spine density in *Fabp4* KO mice

The spine density on apical dendrites of pyramidal neurons has been found to be increased in layers II–III and layer V of the temporal lobe in individuals with ASD (Hutsler and Zhang, 2010). To investigate the effects of *Fabp4* loss-of-function, we analysed spine density in the brains of 4-week-old *Fabp4* KO mice. The spine density on apical dendrites of pyramidal neurons was significantly increased in layers II–III and layer V in the temporal cortex of *Fabp4* KO mice compared to that of their WT littermates (Fig. 4A and B). We obtained similar results in 8-week-old *Fabp4* KO mice (Supplementary Fig. 6). These results indicate that *Fabp4* KO mice also emulate ASD-like phenotypes with respect to spine histology. Next, we morphologically classified the dendritic spines into five categories: filopodia, thin, stubby, mushroom and branched. Four-week-old *Fabp4* KO mice showed significantly fewer mushroom spines (mature form) with a concomitant increase in the number of filopodia spines (immature) (Fig. 4C), suggesting that a systemic loss of Fabp4 affects the maturation of spines in the brain. However, spine analysis of brain regions other than the temporal cortex is required.

Abnormalities in the fatty acid composition of the brain and peripherals in *Fabp4* KO mice

To investigate the effects of *Fabp4* loss-of-function on the FA composition in the cortex, we measured the FAs in the phospholipids in the cortex of 4-week-old *Fabp4* KO mice. The percentage ratios of arachidonic acid ($20:4n - 6$) and docosahexaenoic acid ($22:6n - 3$), and the percentage of $n - 6$ polyunsaturated fatty acid, $n - 3$ polyunsaturated fatty acid and total polyunsaturated fatty acid ($n - 3$ polyunsaturated fatty acid $+ n - 6$ polyunsaturated fatty acid) in total FAs were found to increase in the cortex of *Fabp4* KO mice. On the other hand, the percentages of palmitic acid (16:0), palmitoleic acid ($16:1 n - 7$), vaccenic acid ($18:1 n - 7$) and lignoceric acid (24:0) in total FAs were decreased in the cortex of *Fabp4* KO mice (Fig. 4D). No significant differences were observed in the percentages of other FAs in total FAs (Supplementary Fig. 7).

We also examined the FA composition in the erythrocyte membrane fractions (RBC) and plasma. The percentages of linoleic acid ($18:2n - 6$, LA) and alpha-linolenic acid ($18:3n - 3$) in the total FAs were increased and the percentages of docosatetraenoic acid ($22:4n - 6$) and nervonic acid ($24:1n - 9$) in the total FAs were decreased in *Fabp4* KO mice (Supplementary Table 10). The percentage of docosapentaenoic acid ($22:5n - 3$) in the total FAs was increased in the plasma of the gene-deficient mice (Supplementary Table 10).

Collectively, the loss-of-function of the *Fabp4* gene can elicit changes in the FA composition in the phospholipids both, in the brain and the peripherals, suggesting that Fabp4/FABP4 may play a role in lipid dynamics. However, the altered FA species varied between tissues.

Discussion

In the present study, we focused on the 'adipo-brain axis' as a potential pathophysiology of ASD by examining the serum levels of adipokines and other metabolic markers. Genome-wide association studies have repeatedly reported on the overlap between genetic risk variants in ASD and obesity (Bachmann-Gagescu *et al.*, 2010; Walters *et al.*, 2010; Shinawi *et al.*, 2011; Lee *et al.*, 2012; Sharma *et al.*, 2013; Cortes and Wevrick, 2018; Grove *et al.*, 2019). In addition, a low birth weight has been reported to increase the risk of ASD (Schendel and Bhasin, 2008; Lampi *et al.*, 2012).

We found here that the age-dependent trajectories of adipokine levels were different between ASD and TD children. In particular, the FABP4 levels were found to be significantly lower in ASD children than in TD children in early childhood (2–6 years old). In addition, we have obtained data for the potential of FABP4 as a pathogenetic underpinning factor and an early diagnostic biomarker for ASD.

Regarding the mechanistic role of FABP4 in ASD, we performed exon resequencing analysis of this gene. As a result, two novel and functional variants of the *FABP4* gene were identified, although they were rare. In a previous large-scale exome sequencing study, a *de novo* missense variant in *FABP4* was also found in an individual with ASD (Satterstrom *et al.*, 2020). Moreover, in the same study, 102 risk genes of ASD were identified by exome sequencing, most of which were involved in synaptic functions and gene expression regulation (Satterstrom *et al.*, 2020). The protein–protein interaction network between FABP4 and these 102 candidates revealed that FABP4 interacts with CREBBP, MED13L, PTEN and NCOA1 (Supplementary Fig. 8), which in turn interact with other proteins. This suggests a potential role of FABP4-related network in the manifestation of ASD pathogenesis/phenotype, at least in a subset of ASD.

To corroborate the genetic contribution of *FABP4* to the pathogenesis of ASD, we analysed phenotypes of *Fabp4* gene-disrupted mice. *Fabp4* KO mice exhibited deficits in social behaviour (Fig. 3A and B), in accordance with previous studies in other ASD mouse models
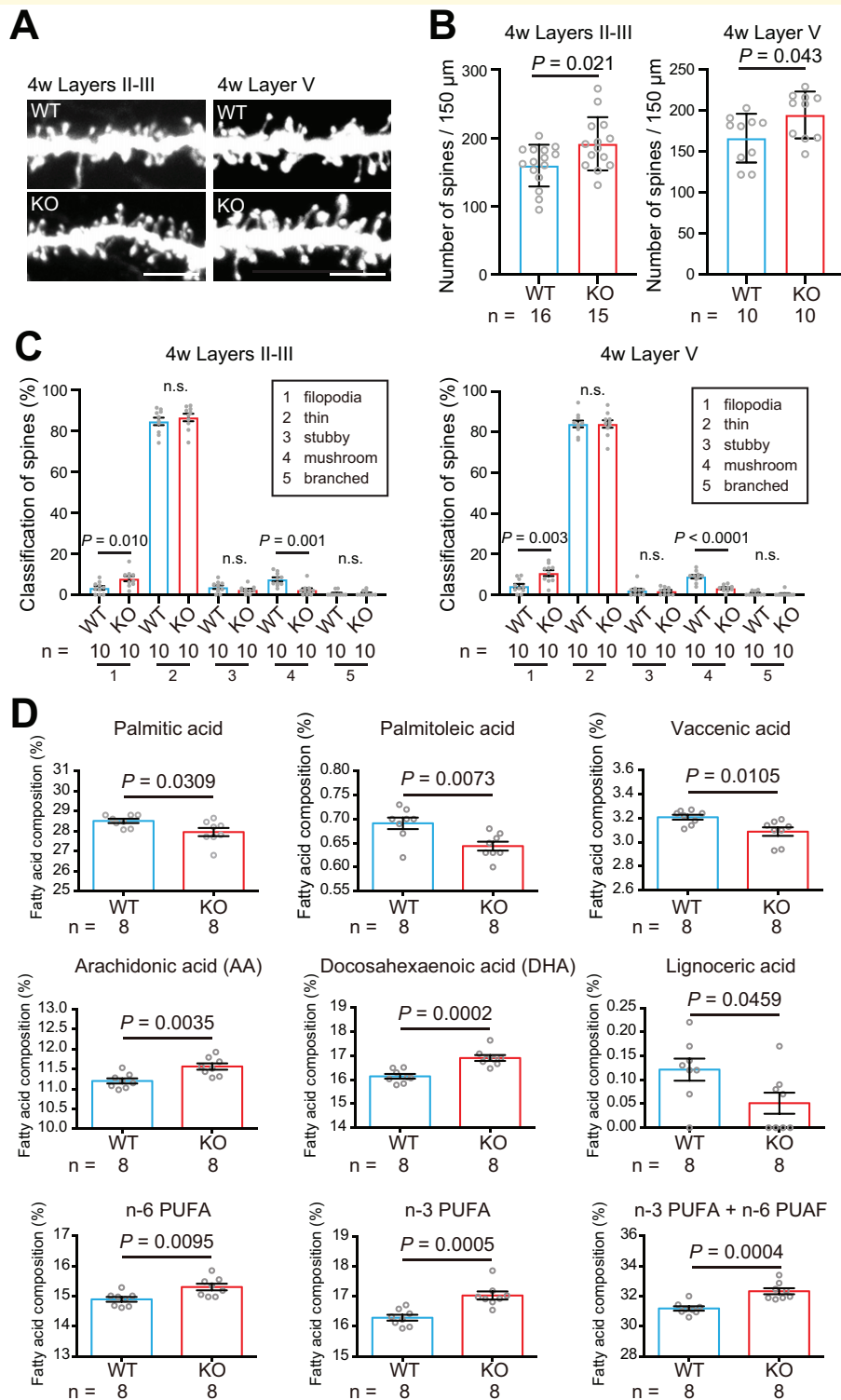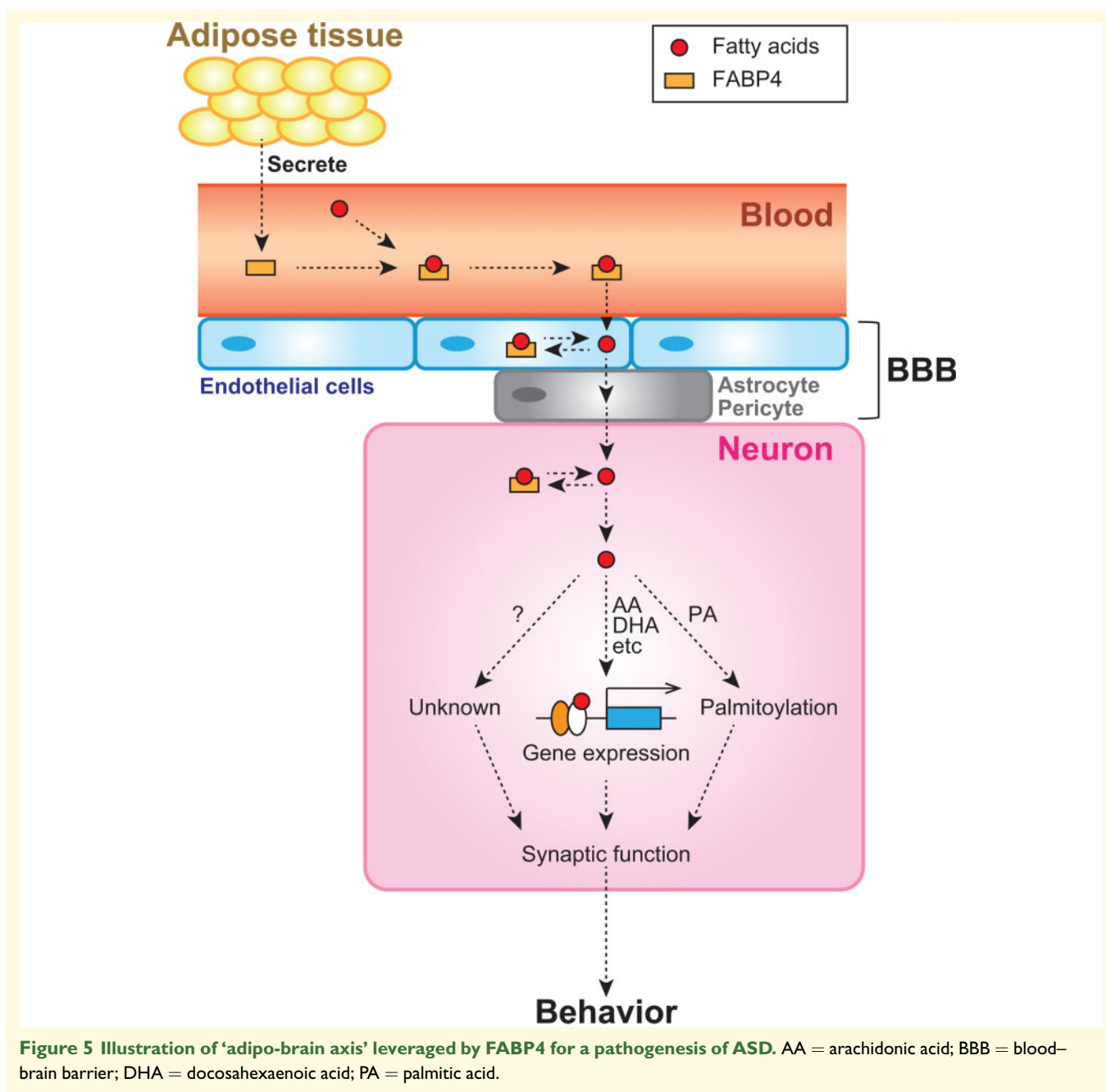
Figure 4 Spine density and FA composition of the cortex of *Fabp4* KO mice. (**A, B**) Spine density on apical dendrites in layers II–III and layer V of the temporal cortex at 4 weeks. *P*-values were calculated using unpaired *t*-tests. Scale bar: 5 μm (**C**) Morphological classification of spines on apical dendrites (filopodia, thin, stubby, mushroom and branched). *P*-values were calculated using unpaired *t*-tests. (**D**) FA composition in the cortex at 4 weeks. *P*-values were calculated using two-tailed Mann–Whitney *U* tests. PUFA, polyunsaturated fatty acid.

(e.g. *Shank3* haploinsufficient mice, *Syngap1* haploinsufficient mice and *Chd8* haploinsufficient mice) (Bozdagi *et al.*, 2010; Berryer *et al.*, 2016; Katayama *et al.*, 2016).

Fabp4 KO mice displayed an increased density of immature spines. It is worth noting that this spine phenotype is similar to the phenotype of *Fmr1* KO mice modelling

Figure 5 Illustration of 'adipo-brain axis' leveraged by FABP4 for a pathogenesis of ASD. AA = arachidonic acid; BBB = blood–brain barrier; DHA = docosahexaenoic acid; PA = palmitic acid.

ASD (Galvez and Greenough, 2005). Collectively, these results indicate that the *Fabp4* KO mice displayed ASD-like features and may therefore be useful as a new mouse model for ASD.

The cortex of *Fabp4* KO mice showed abnormalities in terms of FA composition, including significant increases in docosahexaenoic acid and arachidonic acid. Arachidonic acid and docosahexaenoic acid are known to function as endogenous ligands of the nuclear receptor peroxisome proliferator-activated receptor (Ppar) (Harmon *et al.*, 2011), the activation of which has been reported to increase spine density by regulating downstream genes (Brodbeck *et al.*, 2008; Patel *et al.*, 2018).

The over-activation of Ppar elicited by an increase in the arachidonic acid and docosahexaenoic acid contents in the cortex of *Fabp4* KO animals may result in abnormal spine formation. On the other hand, palmitic acid levels were decreased in the cortex of *Fabp4* KO mice. palmitic acid is involved in the *S*-palmitoylation of multiple synaptic proteins (Zareba-Koziol *et al.*, 2018). Thus, the reduction of palmitic acid in the cortex of *Fabp4* KO mice may also play a role in abnormal spine formation.

The dysregulated transport of FAs from the blood to the brain may play a crucial role in the abnormal composition of FA in *Fabp4* KO mice, and potentially in ASD pathophysiology. It has been reported that FABP5,

another member of the FABP superfamily, is expressed in brain endothelial cells and is involved in the uptake and subsequent blood–brain barrier (BBB) transport of docosahexaenoic acid (Pan *et al.*, 2015). FABP4 is expressed in the same cell population (Elmasri *et al.*, 2009). Therefore, we speculate that FABP4 may also contribute to the transport of FA across the BBB and play a role in ASD pathogenesis.

Our previous studies showed that genetic variations of the brain-expressed *FABP* genes (*FABP3*, *FABP5* and *FABP7*) are involved in the pathogenesis of schizophrenia and ASD (Watanabe *et al.*, 2007; Iwayama *et al.*, 2010; Maekawa *et al.*, 2010; Shimamoto *et al.*, 2014). Some variants in these genes affected ligand-binding properties (Shimamoto *et al.*, 2014). The current study also found that a missense variant of *FABP4* affects ligand-binding properties. Thus, we speculate that peripheral FABP4 may contribute to the pathogenesis of ASD in an indirect manner by altering the fatty acid composition in the brain.

With respect to the lowered serum levels of FABP4 in ASD, environmental factors are likely to play a substantial role, given the rarity of functional variants and no significant genome-wide association study signal in the *FABP4* gene locus (Grove *et al.*, 2019). It has been shown that low birth weight, prematurity and 'small for gestational age' increase the risk for ASD (Schendel and Bhasin, 2008; Lampi *et al.*, 2012). In a mouse model, an abnormal premature leptin surge was observed in offspring that had experienced malnutrition *in utero* (Yura *et al.*, 2005). Considering the links of abnormal *in utero* growth to ASD and to aberrant adipose tissue development, it would be an important future issue to retrospectively examine whether ASD children with low FABP4 levels suffered from malnutrition in foetal stage.

There are several limitations to the present study. First, the sample size used to evaluate the serum concentration of FABP4 protein was relatively small in the current study. Therefore, testing the FABP4 levels in a larger sample size should help us to clarify the clinical or physiological nature of ASD with lowered FABP4. Second, our results were obtained only from Japanese sample sets. Since there are differences in adipose tissue development between different races (Heymsfield *et al.*, 2016), the examination of other ethnic samples, as well as with larger sizes, will be needed to establish serum FABP4 levels as a reliable and universal biomarker. Third, the mechanism for the existence of a time window of lowered FABP4 levels in ASD remains unknown. Fourth, regarding the role of FABP4, the details of the 'adipo-brain axis' have yet to be elucidated. To address the third and fourth issues, the generation and analysis of conditional knockout mice of *Fabp4* in a spatio (tissue-specific)-temporal (developmental stage-specific) manner will be helpful. It will also be interesting to study whether the alterations in FA composition observed in *Fabp4* KO mice are also found in the brains of ASD patients. Lastly, aberrant dendrite morphology was reported in the postmortem brain from subjects with ASD (Raymond *et al.*, 1995; Mukaetova-Ladinska *et al.*, 2004) and in the model animals of ASD including *Fmr1* KO mice (Thomas *et al.*, 2008), CGG knock-in mice with expanded CGG repeats in the 5'-UTR of the *Fmr1* gene (Berman *et al.*, 2012) and *Mecp2*-deficient mice (Belichenko *et al.*, 2009; Nguyen *et al.*, 2012). Therefore, detailed morphological analysis of dendrites and spines in the different cortical regions of *Fabp4* KO mice remains an important issue for the future study.

In summary, in this study, the development of adipose tissue was found to be dysregulated in ASD children, as exemplified by the differential trajectories of serum adipokine levels between ASD and TD subjects. Importantly, this indicated that FABP4 may be a novel player in ASD pathogenesis and a useful biomarker for ASD at early stages, shaping the role of 'adipo-brain axis' in ASD (Fig. 5). Although the replication of the present finding will be necessary, it would also be useful to perform a prospective cohort study on newborns to examine whether the levels of FABP4 at birth can be used to predict the future manifestation of ASD.

Supplementary material

Supplementary material is available at *Brain Communications* online.

Acknowledgements

Funding

Competing interests

The authors report no competing interests.

References

Aeberli I, Beljean N, Lehmann R, l'Allemand D, Spinas GA, Zimmermann MB. The increase of fatty acid-binding protein aP2 in overweight and obese children: interactions with dietary fat and impact on measures of subclinical inflammation. Int J Obes 2008; 32: 1513–20.

Ashwood P, Krakowiak P, Hertz-Picciotto I, Hansen R, Pessah IN, Van de Water J. Associations of impaired behaviors with elevated plasma chemokines in autism spectrum disorders. J Neuroimmunol 2011; 232: 196–9.

Ashwood P, Kwong C, Hansen R, Hertz-Picciotto I, Croen L, Krakowiak P, et al. Brief report: plasma leptin levels are elevated in autism: association with early onset phenotype? J Autism Dev Disord 2008; 38: 169–75.

Bachmann-Gagescu R, Mefford HC, Cowan C, Glew GM, Hing AV, Wallace S, et al. Recurrent 200-kb deletions of 16p11.2 that include the SH2B1 gene are associated with developmental delay and obesity. Genet Med 2010; 12: 641–7.

Balan S, Iwayama Y, Maekawa M, Toyota T, Ohnishi T, Toyoshima M, et al. Exon resequencing of H3K9 methyltransferase complex genes, EHMT1, EHTM2 and WIZ, in Japanese autism subjects. Mol Autism 2014; 5: 49.

Behm-Ansmant I, Kashima I, Rehwinkel J, Sauliere J, Wittkopp N, Izaurralde E. mRNA quality control: an ancient machinery recognizes and degrades mRNAs with nonsense codons. FEBS Lett 2007; 581: 2845–53.

Belichenko PV, Wright EE, Belichenko NP, Masliah E, Li HH, Mobley WC, et al. Widespread changes in dendritic and axonal morphology in Mecp2-mutant mouse models of Rett syndrome: evidence for disruption of neuronal networks. J Comp Neurol 2009; 514: 240–58.

Berman RF, Murray KD, Arque G, Hunsaker MR, Wenzel HJ. Abnormal dendrite and spine morphology in primary visual cortex in the CGG knock-in mouse model of the fragile X premutation. Epilepsia 2012; 53: 150–60.

Berryer MH, Chattopadhyaya B, Xing P, Riebe I, Bosoi C, Sanon N, et al. Decrease of SYNGAP1 in GABAergic cells impairs inhibitory synapse connectivity, synaptic inhibition and cognitive function. Nat Commun 2016; 7: 13340.

Blardi P, de Lalla A, Ceccatelli L, Vanessa G, Auteri A, Hayek J. Variations of plasma leptin and adiponectin levels in autistic patients. Neurosci Lett 2010; 479: 54–7.

Bligh EG, Dyer WJ. A rapid method of total lipid extraction and purification. Can J Biochem Physiol 1959; 37: 911–7.

Bozdagi O, Sakurai T, Papapetrou D, Wang X, Dickstein DL, Takahashi N, et al. Haploinsufficiency of the autism-associated Shank3 gene leads to deficits in synaptic function, social interaction, and social communication. Mol Autism 2010; 1: 15.

Brodbeck J, Balestra ME, Saunders AM, Roses AD, Mahley RW, Huang Y. Rosiglitazone increases dendritic spine density and rescues spine loss caused by apolipoprotein E4 in primary cortical neurons. Proc Natl Acad Sci USA 2008; 105: 1343–6.

Cortes HD, Wevrick R. Genetic analysis of very obese children with autism spectrum disorder. Mol Genet Genomics 2018; 293: 725–36.

Courchesne E, Campbell K, Solso S. Brain growth across the life span in autism: age-specific changes in anatomical pathology. Brain Res 2011; 1380: 138–45.

de la Torre-Ubieta L, Won HJ, Stein JL, Geschwind DH. Advancing the understanding of autism disease mechanisms through genetics. Nat Med 2016; 22: 345–61.

Dencker M, Danielson A, Karlsson MK, Wollmer P, Andersen LB, Thorsson O. Total body fat, abdominal fat, body fat distribution and surrogate markers for health related to adipocyte fatty acid-binding protein (FABP4) in children. J Pediatr Endocrinol Metab 2017; 30: 375–82.

Elmasri H, Karaaslan C, Teper Y, Ghelfi E, Weng M, Ince TA, et al. Fatty acid binding protein 4 is a target of VEGF and a regulator of cell proliferation in endothelial cells. FASEB J 2009; 23: 3865–73.

Esposito G, Hiroi N, Scattoni ML. Cry, baby, cry: expression of distress as a biomarker and modulator in autism spectrum disorder. Int J Neuropsychopharmacol 2017; 20: 498–503.

Falkmer T, Anderson K, Falkmer M, Horlin C. Diagnostic procedures in autism spectrum disorders: a systematic literature review. Eur Child Adolesc Psychiatry 2013; 22: 329–40.

Fujita-Shimizu A, Suzuki K, Nakamura K, Miyachi T, Matsuzaki H, Kajizuka M, et al. Decreased serum levels of adiponectin in subjects with autism. Prog Neuropsychopharmacol Biol Psychiatry 2010; 34: 455–8.

Furuhashi M, Hotamisligil GS. Fatty acid-binding proteins: role in metabolic diseases and potential as drug targets. Nat Rev Drug Discov 2008; 7: 489–503.

Galvez R, Greenough WT. Sequence of abnormal dendritic spine development in primary somatosensory cortex of a mouse model of the fragile X mental retardation syndrome. Am J Med Genet A 2005; 135A: 155–60.

Gillilan RE, Ayers SD, Noy N. Structural basis for activation of fatty acid-binding protein 4. J Mol Biol 2007; 372: 1246–60.

Grove J, Ripke S, Als TD, Mattheisen M, Walters RK, Won H, et al.; Autism Spectrum Disorder Working Group of the Psychiatric Genomics Consortium. Identification of common genetic risk variants for autism spectrum disorder. Nat Genet 2019; 51: 431–44.

Habib A, Harris L, Pollick F, Melville C. A meta-analysis of working memory in individuals with autism spectrum disorders. PLoS One 2019; 14: e0216198.

Harmon GS, Lam MT, Glass CK. PPARs and lipid ligands in inflammation and metabolism. Chem Rev 2011; 111: 6321–40.

Heymsfield SB, Peterson CM, Thomas DM, Heo M, Schuna JM. Why are there race/ethnic differences in adult body mass index-adiposity relationships? A quantitative critical review. Obes Rev 2016; 17: 262–75.

Hotamisligil GS, Johnson RS, Distel RJ, Ellis R, Papaioannou VE, Spiegelman BM. Uncoupling of obesity from insulin resistance through a targeted mutation in aP2, the adipocyte fatty acid binding protein. Science 1996; 274: 1377–9.

Hutsler JJ, Zhang H. Increased dendritic spine densities on cortical projection neurons in autism spectrum disorders. Brain Res 2010; 1309: 83–94.

Iwayama Y, Hattori E, Maekawa M, Yamada K, Toyota T, Ohnishi T, et al. Association analyses between brain-expressed fatty-acid binding protein (FABP) genes and schizophrenia and bipolar disorder. Am J Med Genet B 2010; 153B: 484–93.

Katayama Y, Nishiyama M, Shoji H, Ohkawa Y, Kawamura A, Sato T, et al. CHD8 haploinsufficiency results in autistic-like phenotypes in mice. Nature 2016; 537: 675–9.

Krzystek-Korpacka M, Patryn E, Bednarz-Misa I, Mierzchala M, Hotowy K, Czapinska E, et al. Circulating adipocyte fatty acid-binding protein, juvenile obesity, and metabolic syndrome. J Pediatr Endocrinol Metab 2011; 24: 921–8.

Kurosaki T, Maquat LE. Nonsense-mediated mRNA decay in humans at a glance. J Cell Sci 2016; 129: 461–7.

Lai MC, Lombardo MV, Baron-Cohen S. Autism. Lancet 2014; 383: 896–910.

Lampi KM, Lehtonen L, Tran PL, Suominen A, Lehti V, Banerjee PN, et al. Risk of autism spectrum disorders in low birth weight and small for gestational age infants. J Pediatr 2012; 161: 830–6.

Le Couteur A, Haden G, Hammal D, McConachie H. Diagnosing autism spectrum disorders in pre-school children using two standardised assessment instruments: the ADI-R and the ADOS. J Autism Dev Disord 2008; 38: 362–72.

Lee AW, Hengstler H, Schwald K, Berriel-Diaz M, Loreth D, Kirsch M, et al. Functional inactivation of the genome-wide association study obesity gene neuronal growth regulator 1 in mice causes a body mass phenotype. PLoS One 2012; 7: e41537.

Lord C, Rutter M, Le Couteur A. Autism Diagnostic Interview-Revised: a revised version of a diagnostic interview for caregivers of individuals with possible pervasive developmental disorders. J Autism Dev Disord 1994; 24: 659–85.

Luo L, Liu M. Adipose tissue in control of metabolism. J Endocrinol 2016; 231: R77–R99.

Maekawa M, Iwayama Y, Arai R, Nakamura K, Ohnishi T, Toyota T, et al. Polymorphism screening of brain-expressed FABP7, 5 and 3 genes and association studies in autism and schizophrenia in Japanese subjects. J Hum Genet 2010; 55: 127–30.

Maekawa M, Yamada K, Toyoshima M, Ohnishi T, Iwayama Y, Shimamoto C, et al. Utility of scalp hair follicles as a novel source of biomarker genes for psychiatric illnesses. Biol Psychiatry 2015; 78: 116–25.

Maquat LE. Nonsense-mediated mRNA decay in mammals. J Cell Sci 2005; 118: 1773–6.

Mataga N, Mizuguchi Y, Hensch TK. Experience-dependent pruning of dendritic spines in visual cortex by tissue plasminogen activator. Neuron 2004; 44: 1031–41.

McGrath J, Johnson K, Ecker C, O'Hanlon E, Gill M, Gallagher L, et al. Atypical visuospatial processing in autism: insights from functional connectivity analysis. Autism Res 2012; 5: 314–30.

Mukaetova-Ladinska EB, Arnold H, Jaros E, Perry R, Perry E. Depletion of MAP2 expression and laminar cytoarchitectonic changes in dorsolateral prefrontal cortex in adult autistic individuals. Neuropathol Appl Neurobiol 2004; 30: 615–23.

Mukai H, Hatanaka Y, Mitsuhashi K, Hojo Y, Komatsuzaki Y, Sato R, et al. Automated analysis of spines from confocal laser microscopy images: application to the discrimination of androgen and estrogen effects on spinogenesis. Cereb Cortex 2011; 21: 2704–11.

Nguyen MV, Du F, Felice CA, Shan X, Nigam A, Mandel G, et al. MeCP2 is critical for maintaining mature neuronal networks and global brain anatomy during late stages of postnatal brain development and in the mature adult brain. J Neurosci 2012; 32: 10021–34.

Ohnishi T, Watanabe A, Ohba H, Iwayama Y, Maekawa M, Yoshikawa T. Behavioral analyses of transgenic mice harboring bipolar disorder candidate genes, IMPA1 and IMPA2. Neurosci Res 2010; 67: 86–94.

Pan Y, Scanlon MJ, Owada Y, Yamamoto Y, Porter CJ, Nicolazzo JA. Fatty acid-binding protein 5 facilitates the blood-brain barrier transport of docosahexaenoic acid. Mol Pharmaceutics 2015; 12: 4375–85.

Parimisetty A, Dorsemans A-C, Awada R, Ravanan P, Diotel N, Lefebvre d'Hellencourt C. Secret talk between adipose tissue and central nervous system via secreted factors-an emerging frontier in the neurodegenerative research. J Neuroinflammation 2016; 13:67.

Patel D, Roy A, Kundu M, Jana M, Luan C-H, Gonzalez FJ, et al. Aspirin binds to PPARa to stimulate hippocampal plasticity and protect memory. Proc Natl Acad Sci USA 2018; 115: E7408–E17.

Prentice KJ, Saksi J, Hotamisligil GS. Adipokine FABP4 integrates energy stores and counterregulatory metabolic responses. J Lipid Res 2019; 60: 734–40.

Raymond GV, Bauman ML, Kemper TL. Hippocampus in autism: a Golgi analysis. Acta Neuropathol 1995; 91: 117–9.

Rylaarsdam L, Guemez-Gamboa A. Genetic causes and modifiers of autism spectrum disorder. Front Cell Neurosci 2019; 13: 385.

Satterstrom FK, Kosmicki JA, Wang J, Breen MS, De Rubeis S, An JY, et al. Large-scale exome sequencing study implicates both developmental and functional changes in the neurobiology of autism. Cell 2020; 180: 568–84 e23.

Schendel D, Bhasin TK. Birth weight and gestational age characteristics of children with autism, including a comparison with other developmental disabilities. Pediatrics 2008; 121: 1155–64.

Sharma JR, Arieff Z, Gameeldien H, Davids M, Kaur M, van der Merwe L. Association analysis of two single-nucleotide polymorphisms of the RELN gene with autism in the South African population. Genet Test Mol Biomarkers 2013; 17: 93–8.

Shimamoto C, Ohnishi T, Maekawa M, Watanabe A, Ohba H, Arai R, et al. Functional characterization of FABP3, 5 and 7 gene variants identified in schizophrenia and autism spectrum disorder and mouse behavioral studies. Hum Mol Genet 2014; 23: 6495–511.

Shinawi M, Sahoo T, Maranda B, Skinner SA, Skinner C, Chinault C, et al. 11p14.1 microdeletions associated with ADHD, autism, developmental delay, and obesity. Am J Med Genet A 2011; 155: 1272–80.

Thomas CC, Combe CL, Dyar KA, Inglis FM. Modest alterations in patterns of motor neuron dendrite morphology in the Fmr1 knockout mouse model for fragile X. Int J Dev Neurosci 2008; 26: 805–11.

Walters RG, Jacquemont S, Valsesia A, de Smith AJ, Martinet D, Andersson J, et al. A new highly penetrant form of obesity due to deletions on chromosome 16p11.2. Nature 2010; 463: 671–5.

Watanabe A, Toyota T, Owada Y, Hayashi T, Iwayama Y, Matsumata M, et al. Fabp7 maps to a quantitative trait locus for a schizophrenia endophenotype. PLoS Biol 2007; 5: e297.

Weintraub K. Autism counts. Nature 2011; 479: 22–4.

Wolff JJ, Gu H, Gerig G, Elison JT, Styner M, Gouttard S, et al. the IBIS Network. Differences in white matter fiber tract development present from 6 to 24 months in infants with autism. Am J Psychiatry 2012; 169: 589–600.

Yura S, Itoh H, Sagawa N, Yamamoto H, Masuzaki H, Nakao K, et al. Role of premature leptin surge in obesity resulting from intrauterine undernutrition. Cell Metab 2005; 1: 371–8.

Zareba-Koziol M, Figiel I, Bartkowiak-Kaczmarek A, Wlodarczyk J. Insights into protein S-palmitoylation in synaptic plasticity and neurological disorders: potential and limitations of methods for detection and analysis. Front Mol Neurosci 2018; 11:175.

Zimmerman AW, Veerkamp JH. New insights into the structure and function of fatty acid-binding proteins. Cell Mol Life Sci 2002; 59: 1096–116.